Journal of Imaging Science and Technology® 57(1): 010501-1–010501-7, 2013.

Improvements of Nonuniform Optical Response for QR-LPD

Chang-Jing Yang and Yung-Fang Chen
Department of Communication Engineering, National Central University, Taiwan 320, R.O.C
E-mail: yfchen@ce.ncu.edu.tw

Abstract. *A quick-response liquid powder display (QR-LPD) is a favorable candidate for flexible electronic paper since it provides an affordable plastic panel fabrication. However, significant image noise is perceived on QR-LPDs. In this article, we discuss the root causes of nonuniform optical response and powder clustering. We propose an image compensation system to improve the nonuniform optical response. The experiment results show improvements in the mean-square signal-to-noise ratio of over 8.6 dB, with an average improvement of 4.6 dB. © 2013 Society for Imaging Science and Technology.*
[DOI: 10.2352/J.ImagingSci.Technol.2013.57.1.010501]

INTRODUCTION

A quick-response liquid powder display (QR-LPD) is a passive display based on the movement of charged pigment powders suspended in air under an external electric field. Pigment powders with diameters of 0.1–20 μm are placed into pixels surrounded by ribs, and are sandwiched between two electrodes at a distance of 50–100 μm.[1] Two types of colored powder have been developed for QR-LPDs: one is white and the other black. When the two powders are mixed in a QR-LPD, the white powders become charged negatively and the black powders charged positively.[2] The charging mechanism of powders in the electrification of particles is mainly a surface-dominated process,[3−7] and the charge-holding capacity related to the relaxation time of the discharge depends on the material characteristics.

The charging mechanism of powders is mainly surface-dominated electrification, and the material characteristics determine the charge-holding capacity. The basic charging mechanism of a QR-LPD is illustrated in Figure 1. The powders have an initial residual charge as the voltage is flipped, as shown in Fig. 1(a). When the removal force by the applied electric field, which is given by $F = qE$ (where q is the charge of the powder and E is the electric field), exceeds the attractive force, the powders begin to move. As shown in Fig. 1(b), frictional charging occurs when the powders come into contact with each other. The contact area and the relative velocity determine the triboelectric charge of the powders. When the powders arrive at the electrode with an opposite charge, as shown in Fig. 1(c), the powders may also pick up additional charge by tribocharging. The powder charge accumulates when the image refreshes, and leaks slowly when the image is held.

The major difference between a QR-LPD and conventional electrophoretic displays (EPDs) is that the powder moves in air for the former and in fluid for the latter. A QR-LPD has the superior characteristics of a well-defined threshold and a fast response time, and can be easily operated using passive-matrix driving methods.[8] In conventional threshold-less EPDs, an active-matrix backplane plays the important role of being the control switch for applied voltages on pixels. In contrast, a well-defined threshold is able to leave the control switches aside. Only the pixels whose driven voltages are higher than the threshold have sufficient potential energy to be switched. Moreover, in traditional wet-type EPDs, a low optical switching speed is also a major drawback. Because particles move slowly in fluids, the response time is greater than several tens of milliseconds. The storage capacitors of an active-matrix backplane are charged to hold the driving voltages on switching pixels while other lines are being scanned, so multiple lines update simultaneously while writing an image. On the other hand, with a QR-LPD having a response time of less than 0.2 ms, a passive-matrix QR-LPD without storage capacitors achieves an even faster image refreshing rate than an active-matrix EPD. Moreover, multi-line addressing (MLA) and shrunk single-line addressing (SSLA) were proposed to speed up the image refreshing rate for a QR-LPD.[9,10] Constrained non-negative matrix factorization (CNMF) reproduces row and column data matrices, and multiple row lines scan simultaneously while an image is updating. The selected periods are reduced to necessary ones by eliminating the waiting time. However, MLA unavoidably results in decomposition and quantization losses when using fast multi-line scanning.

QR-LPDs are preferred candidates for flexible electronic papers as they permit simple plastic panel fabrication. The high-temperature process inherent in thin-film transistor (TFT) fabrication is difficult to employ in a plastic panel. Because a clear threshold and fast response time yielding a QR-LPD can be easily driven by a passive matrix, a practical fabrication process was illustrated in Ref.1. Hence, a flexible reflective display that is thin and lightweight, and that has low power consumption, fast response time, and low manufacturing cost, is an attainable goal for current display makers.

In this article, we discuss image noises on a QR-LPD. Using a microscopic observation of images with 16 gray levels displayed on a QR-LPD, the root causes of the

Received Jul. 29, 2011; accepted for publication Feb. 14, 2013; published online Apr. 29, 2013.
1062-3701/2013/57(1)/010501/7/$20.00

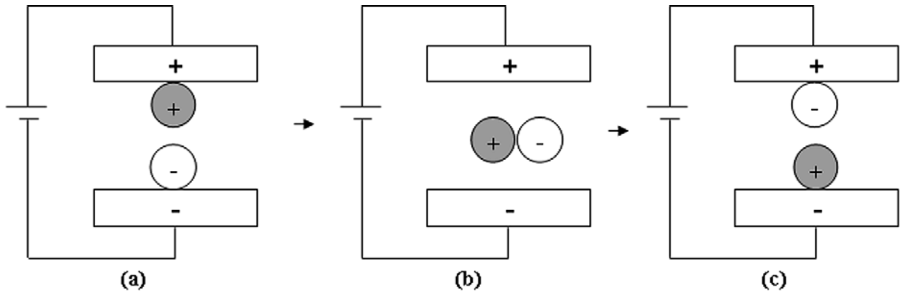

Figure 1. Charging mechanism of a QR-LPD.

image noises are found. Nonuniform optical response and powder clustering become visible while an observer moves close to the image. Currently, there are few articles that discuss the nonuniformity of liquid crystal displays (LCDs). Some articles have discussed the uniformity for backlight dimming of LCDs, and luminance scaling methods have been proposed for the system.[11,12] However, the solutions discussed in the previous works are not suitable when dealing with the nonuniformity of a QR-LPD since the root causes of the problem are different for a QR-LPD and an LCD. Therefore, we propose a fast image compensation system to improve the nonuniform optical response of a QR-LPD. In the experimental results, the mean-square signal-to-noise ratio (MSSNR) improves to a maximum of 8.647 dB, and to an average of 4.662 dB.

OVERVIEW OF QR-LPD OPERATION

A driving waveform triggers the operational procedures of a QR-LPD. Pulse amplitude modulation (PAM), pulse width modulation (PWM), and pulse number modulation (PNM) have generally been utilized to render grayscale on EPDs. Mid-tone images with more than four gray levels have been successfully implemented in Refs.13–15. Initially, the sequence of a driving waveform for a bistable display is to erase the prior image that turns the entire display white. We assume that the white powders with negative charge appear on the observation substrate when a positive electric field is applied; conversely, the black powders with positive charge appear when a negative electric field is applied. Figure 2(a) shows an example of pixel voltages between a QR-LPD column and a row electrode. The first sequence of a driving waveform is powder activation. Considering that white powder appears on the observation substrate when a positive electric field $+E$ is applied, black powder conversely appears with the application of a negative electric field E. A sequence of powder activation utilizes a waveform of f_a cycles per driving waveform, where t_{ap} is the width of positive pulses and t_{an} is the width of negative pulses. When the sign of the pixel voltage changes, the powders migrate to the other electrode, and additional charging mechanisms occurs. The second sequence for clearing a prior image is then performed. Before a new image is updated, the previous image remains on the observation substrate because the display is bistable. In order to achieve a higher contrast ratio, PNM is employed. The pulse width t_c and pulse number n_c determine the

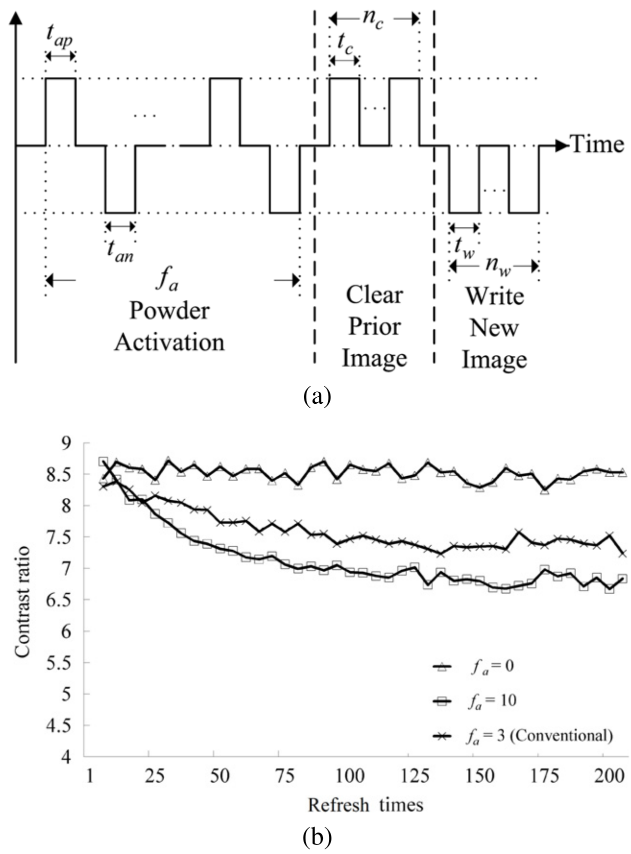

Figure 2. (a) Pixel voltage between a column and a row electrode, (b) contrast ratios driven by pixel voltage of various.

reflectance quality of an image's white background. The final sequence is to update a new image; the pulse width t_w and the pulse number n_w determine the gray level.

In Ref. 16, we discussed the effects of the powder charge of a QR-LPD; there is a significantly effect on the optical performance. With heavy charge powders using the presented waveform, the image force increases. The removing force given by the applied electric field is insufficient to move the powders, and the display achieves a poor optical performance. Therefore, an adaptive sequence of powder activation should be considered for a QR-LPD. Using the presented driving waveform shown in Fig. 2(a), the experiment next added the powder activation sequence to the waveform at which the frequencies with f_a ranged from 0 to 10, having pulse width of t_{ap} and t_{an} equal to 500 μs.

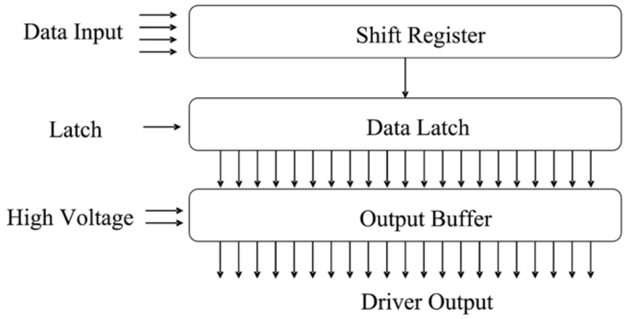

Figure 3. Block diagram of QR-LPD driver.

A required high applied voltage of 70 V was employed with n_c and $n_w = 10$ and t_c and $t_w = 500$ µs. Since the charge of powder is expected to increase, the image was refreshed to more than 200 times on a QR-LPD and the optical responses were recorded. The experimental results of the contrast ratio are shown in Fig. 2(b). With a smaller f_a in the sequence, the contrast ratio was higher than others. Conversely, it achieved a lower contrast ratio when f_a increased. This indicates that the triboelectric charge among powders increases when f_a increases, and accumulates according to the refresh times of images. Slight charging should be employed when images update frequently. Conversely, a strong activation of powder should be used when a QR-LPD is idle for a long period. A long-run test with a slight charge on the QR-LPD was implemented, and a contrast ratio of 5 can remain after an image has been refreshed over 300 000 times.

Figure 3 shows the block diagram of a QR-LPD driver. Encoded data are serially inputted to the shift register. While the latch signal is enabled, the data in the shift register are outputted to the output buffer. The buffer drives the output into the tri-level voltage states of high voltage (HV), middle voltage (MV), and zero voltage (0V) of the driver. For example, in a conventional row-by-row driving scheme, the MV is lower than the threshold voltage of a QR-LPD. The voltage of the selected row and unselected row can be set to HV and MV, respectively, and the voltage of the switched and unswitched columns can be set to 0V and MV, respectively. The pixel voltages of the unselected rows across the electrodes are given by MV–0V or MV–MV, which are lower than the threshold voltage, and those of the active and non-active pixels of the selected rows are given by HV–0V and HV–MV, respectively. The details of the driving method and the electro-optical response of the driving method are further discussed in Ref.17.

The grayscale rendition of a basic row-by-row driving scheme is shown in Figure 4(a). The pulses at a low level denote that the row is unselected and those at a high level denote that the row is selected. The pulse of a column at either a low or a high level denotes that the column is unswitched and switched, respectively. Note that the pulse level does not indicate the voltage level of the row and column, which is the driver operation status. In the previous study,[17] we measured the electro-optical response of a QR-LPD device. The threshold voltage is approximately 35 V. Within an applied voltage below the threshold, the QR-LPD shows a clear threshold; only a few particles move to the opposite electrode, and the contrast increases slightly. When the applied voltage is larger than the threshold, the optical contrast is a function of both the applied voltage and the pulse width. Therefore, voltage levels of 35 V for MV and 70 V for HV are employed. When column data are inputted, only one row is selected. The combination of the pulse levels of the row and the column determines the grayscale of the pixel on a display. The formulation is denoted by $y_{ij} = r_i \wedge c_j$, where y_{ij} is the grayscale of the pixel at the ith row and the jth column. r_i and c_j are the pulse levels of the ith column and jth row, respectively. For example, the grayscale of the pixel across the first column and first row is denoted by $y_{11} = r_1 \wedge c_1$, where r_1 and c_1 are the pulse levels of the first column and first row, respectively. Assume that a QR-LPD is erased to a white image; y_{11} is larger than y_{33} because the driving waveform with fewer pulses is driven.

In Ref. 17, the optical response of QR-LPDs using pulse amplitude modulation (PAM), pulse width modulation (PWM), and pulse number modulation (PNM) have been observed. PNM can achieve better optical contrast than the other driving methods because it can obtain a higher powder density within a pixel, and is attributed to the repulsive force between powders. In the interval between two consecutive driving pulses, the repulsive force moves powders, and more spaces appear among them. When the next driving pulse is applied, more powders squeeze into the spaces. Therefore, a higher powder density within a pixel is gradually achieved using multiple driving pulses. PNM is required to obtain higher optical contrast for driving the QR-LPD, since the maximum optical contrast is insufficient when it is driven by a single pulse. However, the duration of the driving waveform increases along with the number of pulses. The balance between the optical contrast and the image update speed is a trade-off, and requires careful consideration. With multiple pulses in the driving waveform, a lower image update speed is a trade-off for the improved optical contrast. Fig. 4(b) shows experimental results of the contrast ratio as a function of pulse number, and the pulse widths range from 50 to 500 µs. Single pulses of varying amplitudes and widths are used to drive the QR-LPD. Within an applied voltage below the threshold, only a few powders move to the opposite electrode, and the contrast increases slightly. When the applied voltage is larger than the threshold, the optical contrast is a function of the applied voltage and pulse width. A driving waveform with a larger pulse width and larger number of pulses yields a higher contrast ratio. With a pulse width larger than 500 µs, the contrast ratio curves nearly overlapped. Moreover, the optical response curves did not show linearity with respect to pulse widths and pulse numbers. The driving waveform did not yield an obvious increase in the optical contrast when the pulse number was larger than 10.

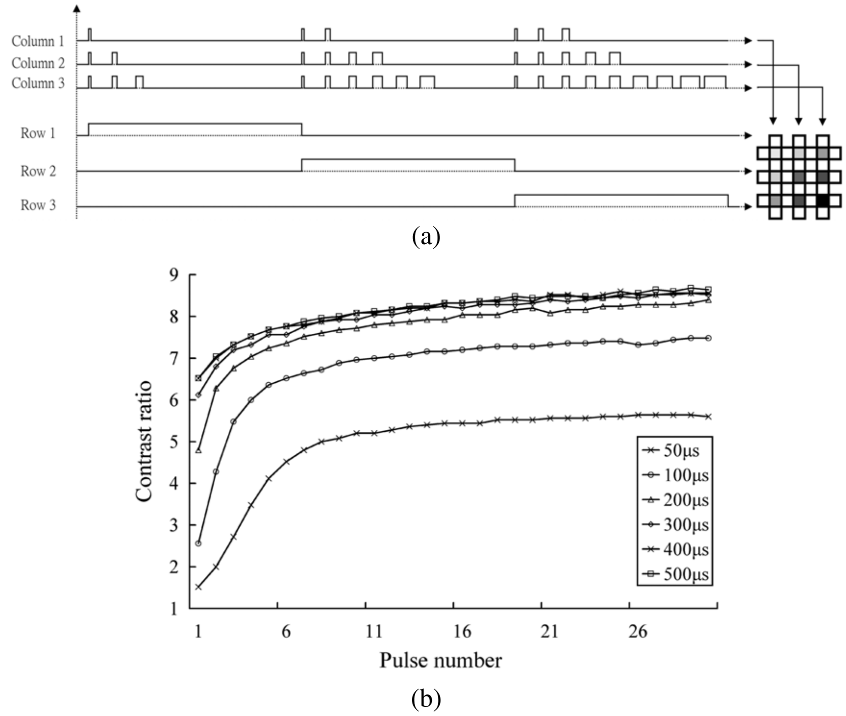

Figure 4. (a) A basic row-by-row driving scheme, (b) electro-optic response of a QR-LPD.

IMAGE NOISE ANALYSIS

Consider the contrast sensitivity function (CSF) of the human vision system. A person who has 20/20 vision can resolve 5 line pairs per mm at a reading distance of 343 mm (30 cycles/degree).[18,19] This implies that an observer should not be able to identify a single dot since a powder diameter of 0.1–20 μm is less than the sensitivity for the human eye. However, by observing the grayscale renditions on a QR-LPD, the images appear to be noisy. For further analysis, Figure 5 shows a microscopic view of a middle gray level on a QR-LPD. The pigment powder distribution in a pixel generates the gray level. Furthermore, the spaces without any pigment powders show a different reflectance and affect the gray level as well. Therefore, the grayscale of a pixel can be represented as a function of black powders, white powders, and spaces without pigment powders. The formulation of the grayscale of a pixel can be represented as $R_p = f(R_B, R_w, R_e; A_B, A_w, A_e)$, where R_B, R_w, and R_e denote the reflectance of black powder, white powder, and empty zone, respectively, and A_B, A_w, and A_e represent the area of black powder, white powder, and empty zone, respectively. Generally, the grayscale can be estimated by

$$\hat{R}_p = (R_B \cdot A_B + R_w \cdot A_w + R_e \cdot A_e)/A, \tag{1}$$

where A is the area of a pixel.

A powerful driving waveform with a large number of pulses and large pulse width is used to drive pixels during the erasing period. This leads to a strong drive on pixels, and does not show much optical difference among pixels at the beginning. However, the nonuniform optical response appears among pixels, and has worsened when the pixels are driven to an opposite progression. It not only induces a gray level error, but also decreases the image contrast on a QR-LPD.

In the manufacturing process of the powders of a QR-LPD, it is difficult for either a crushing or a polymerization method to produce powders of a uniform dimension. Moreover, in the powder filling process, a nozzle scatters powders over a container, and these eventually fall into the cell.[20] The amount of powder is also difficult to control for each pixel. With various dimensions and quantities of powder in pixels surrounded by the ribs, the optical response varies among pixels, which leads to a nonuniform optical response on a QR-LPD.

IMAGE COMPENSATION SYSTEM

We propose an image compensation system to mitigate the nonuniform optical response of a QR-LPD. Figure 6 shows the block diagram of the proposed image compensation system. Initially, a template image with one gray level is delivered to a QR-LPD, and the proposed system then uses a microscope with a high-resolution camera to capture the template image on a QR-LPD. The captured image with multiple cells is divided into several segmented one-cell images. The segmented image should possess sufficient details to know the pigment powder distributions. Next, the normalization process standardizes the light reflection on the display. Because the luminance is not uniform on the panel while capturing the template image, the gray level in the segmented image is scaled to a normalized value of the segmented image. Therefore, each segmented image

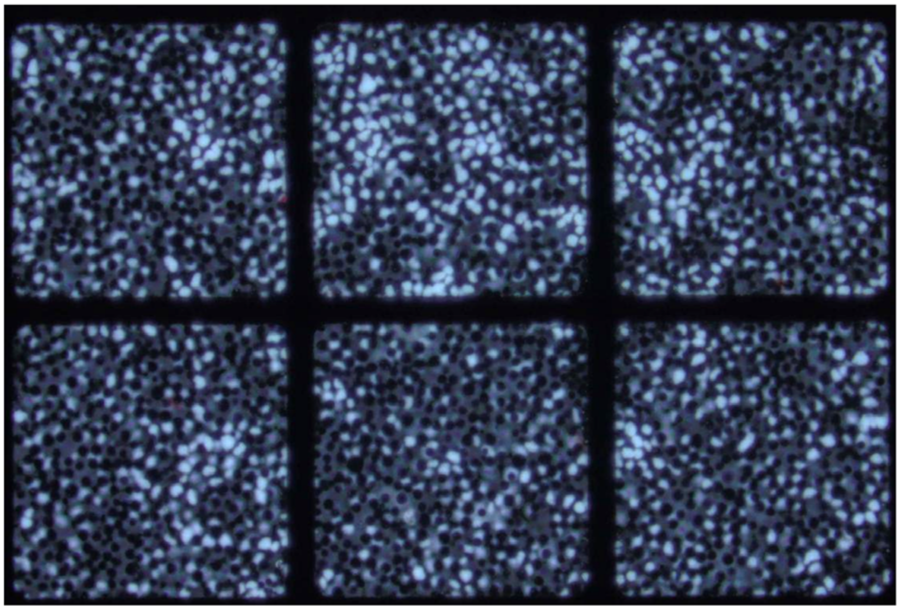

Figure 5. A microscopic view of a middle gray level displayed on QR-LPD.

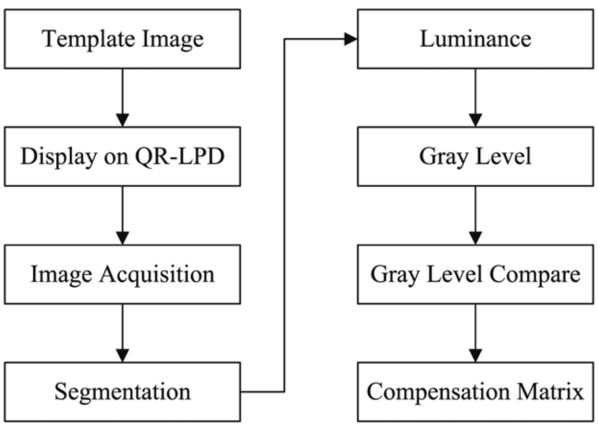

Figure 6. The block diagram of the proposed image compensation.

has a uniform grayscale, and the luminance is normalized accordingly.

The estimation of the gray level of a pixel is based on (2). The grayscale of a pixel is to obtain an average value of the segmented image. By comparing the gray level of the template image and the average gray level of the segmented image, the grayscale error is calculated and a compensation matrix is built. The components of the compensation matrix that represent the grayscale error should be compensated on the pixels.

EXPERIMENTAL RESULTS

The captured image of the middle gray level has 100 pixels, as shown in Figure 7(a). The densities of black and white powders are nonuniform and irregular among pixels. The grayscale distribution is shown in Fig. 7(b). There is a grayscale shift of more than 10% among pixels. The proposed image compensation system calculates the gray level error and generates a compensation matrix, as shown in Fig. 7(c). The captured image after compensation is shown in Figure 8(a), and the grayscale distribution is shown in Fig. 8(b). The error in the grayscale is smaller than the one before the compensation, and the nonuniform optical response is improved. Template images with 16 gray levels are delivered to the proposed system, and we repeat the calculation for each template image. The compensation matrices are generated and the template images with compensation are obtained accordingly.

We use the MSSNR to estimate the image quality, which is given below.

$$MSNR = \frac{\sum_{x=0}^{M-1}\sum_{y=0}^{N-1}\tilde{f}(x,y)^2}{\sum_{x=0}^{M-1}\sum_{y=0}^{N-1}\left[\tilde{f}(x,y)-f(x,y)\right]^2}, \tag{2}$$

where M and N are the number of rows and columns in the image, respectively, and $f(x,y)$ and $\tilde{f}(x,y)$ are the gray levels of the template and the captured image, respectively. Figure 9 shows the MSSNRs of the 16 gray level template images before and after achieving image compensation. The MSSNRs shows a climbing curve when increasing the gray level. A driving waveform with numerous pulses and a large pulse width erases a QR-LPD to a white image before displaying an image, and achieves the highest MSSNR during the erasing period. When a QR-LPD progressively drives to a black image, the nonuniform optical response has become worse; therefore, the MSSNRs decrease accordingly.

The MSSNRs were observed to significantly improve when using the compensation matrices that are generated by the proposed system. Compared to the MSSNRs of the template images before achieving the image compensation, the maximum improvement of the MSSNR is 8.647 dB in

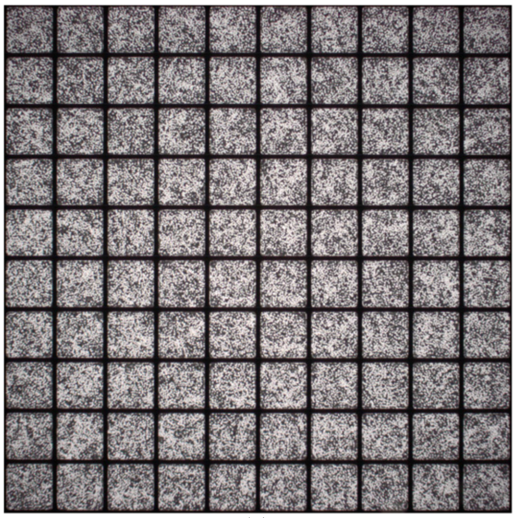

(a)

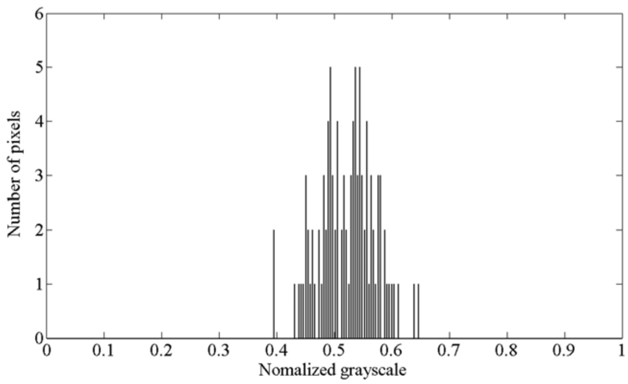

(b)

1	1	1	1	0	0	0	1	1	1
1	3	1	1	0	0	1	0	1	1
1	0	1	1	0	0	0	1	1	3
0	0	0	0	0	0	0	1	1	1
-2	0	0	0	0	0	0	0	0	1
0	0	0	1	0	0	0	1	0	0
0	0	0	1	0	0	0	0	0	1
1	0	0	0	0	0	0	0	1	1
1	-2	0	-2	1	0	0	0	1	1
1	0	0	0	0	0	0	1	0	1

(c)

Figure 7. (a) Captured image of 100 pixels at the middle gray level. (b) Grayscale distribution of the 100 pixels. (c) Compensated matrix.

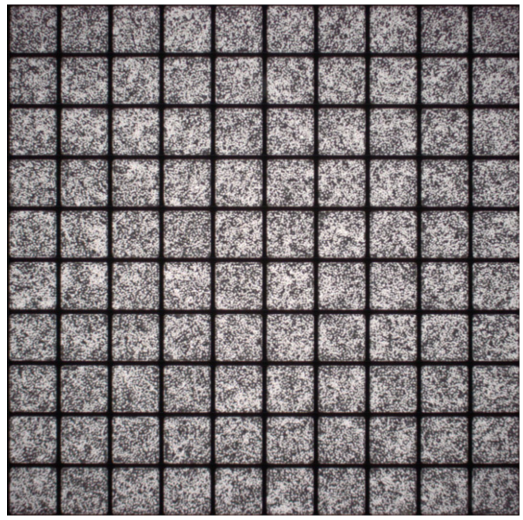

(a)

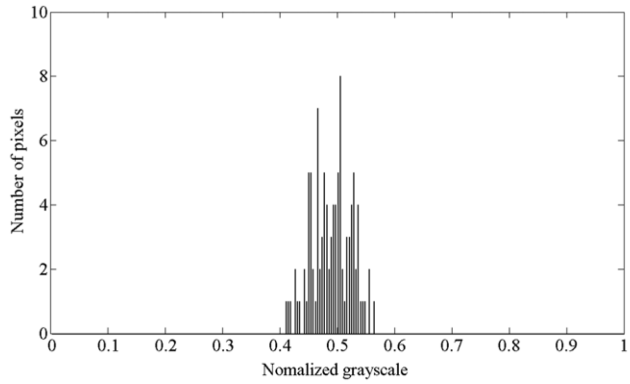

(b)

Figure 8. (a) Captured image after compensation. (b) Grayscale distribution of the captured image.

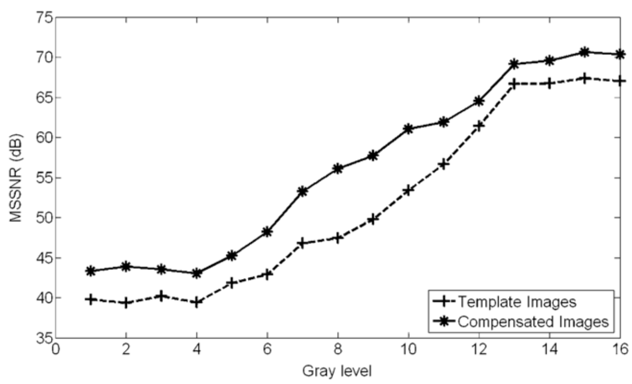

Figure 9. A comparison of the MSSNRs of the template images and the compensated images.

the middle gray level, and 4.662 dB on average. Moreover, we recorded the contrast ratio of an operational test of a QR-LPD, as shown in Figure 10. The experiment result shows that the QR-LPD maintains a stable contrast ratio when an image has been refreshed on a QR-LPD over 15 000 times.

CONCLUSION

In this article, we have discussed image noises on a QR-LPD. We have proposed an image compensation system to mitigate the nonuniform optical response of a QR-LPD. We first discussed the basic charging mechanism and the driving waveform for a QR-LPD. The powder charge of QR-LPD significantly affects the optical performance. With a heavy

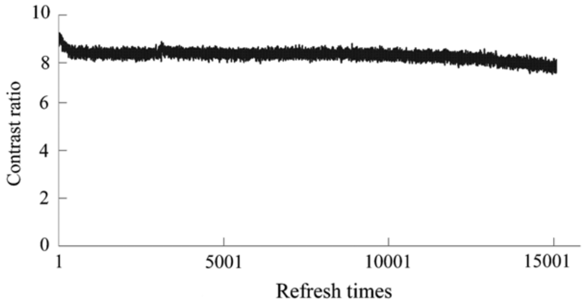

Figure 10. The recorded contrast ratio of a QR-LPD when an image has been refreshed over 15,000 times.

charge of powders using the presented waveform, the image force increased. The removing force given by the applied electric field is insufficient to move the powders, and the display achieves a poor optical performance. Therefore, an adaptive sequence of powder activation should be considered for QR-LPDs. A slight charging should be employed when images update frequently. From performing a microscopic observation of images with 16 gray levels displayed on a QR-LPD, the root causes of the image noises were identified. Nonuniform optical response and powder clustering become visible when an observer moves close to the image, and an image compensation system was proposed to mitigate the nonuniform optical response. The proposed system calculates the gray level error and generates a compensation matrix. In the experimental results, the nonuniformity of the compensated image was mitigated and the MSSNR was improved.

ACKNOWLEDGMENT

The authors would like to thank the National Science Council of the Republic of China, Taiwan, for financially supporting this research under Contract no. NSC 101-2221-E-008-069.

REFERENCES

[1] R. Hattori, S. Yamada, Y. Masuda, and N. Nihei, "A novel bistable reflective display using quick-response liquid powder," J. SID **12**, 75–78 (2004).

[2] N. Kaga and T. Arai, US Patent 7,483,201, Jan. (2009).

[3] J. S. Chang, A. J. Kelly, and J. M. Crowley, *Handbook of Electrostatic Processes* (Macel Dekker, Inc., New York, 1995).

[4] G. S. P. Castle and L. B. Schein, "General model of sphere–sphere insulator contact electrification," J. Electrostatics **36**, 165–173 (1995).

[5] Y. Hoshino, K. Li, D. J. Karunanayake, and T. Hasegawa, "Review of toner-based printing technologies and fundamentals of toner charging mechanism," J. Imaging Sci. Technol. **54**, 1 (2010).

[6] L. B. Schein, "Comparison of toner adhesion theories," J. Imaging Sci. Technol. **53**, 1–8 (2009).

[7] L. B. Schein, "Role of technical innovation in the physics of electrophotography," J. Imaging Sci. Technol. **54**, 1–9 (2010).

[8] Y. Masuda, N. Nihei, R. Sakurai, and R. Hattori, "A reflective-display QR-LPD," J. SID **14**, 443–448 (2006).

[9] S. Kaneko, M. Asakawa, R. Hattori, Y. Masuda, N. Nihei, A. Yokoo, and S. Yamada, "Multiline addressing of quick-response liquid powder display (QR-LPD) using non-negative matrix factorization," *IDW 08*, (2008), pp. 1267–1270.

[10] S. Kaneko, M. Asakawa, R. Hattori, Y. Masuda, N. Nihei, A. Yokoo, and S. Yamada, "Additional speeding-up method of updating time for bistable passive-matrix driven display by shrinking multiline addressing data," *IDW 09*, (2009), pp. 2105–2108.

[11] N. Chang, I. Choi, and H. Shim, "DLS: dynamic backlight luminance scaling of liquid crystal display," IEEE Trans. Very Large Scale Integration Systems **12**, 837–846 (2004).

[12] S. J. Kang and Y. H. Kim, "Image integrity-based gray-level error control for low power liquid crystal displays," IEEE Trans. Consumer Electron **55**, 2401–2406 (2009).

[13] W. C. Kao, J. A. Ye, F. S. Lin, P. Y. Cheng, and R Sprague, "Configurable timing controller design for active matrix electrophoretic display," IEEE Trans. Cons. Electr. **55**, 1–5 (2009).

[14] W. C. Kao, "Electrophoretic display controller integrated with real-time halftoning and partial region update," IEEE J. Disp. Technol. **6**, 36–44 (2010).

[15] S. Yamada, S. Wakuda, and R. Hattori, "Grayscale for QR-LPD," Technical Report of IEICE **103**, 41–44 (2004).

[16] C. J. Yang and Y. F. Chen, "Driving waveform based on powder charge for a quick-response liquid powder display," J. SID **20**, 300–303 (2012).

[17] C. J. Yang and Y. F. Chen, "Programmed driving waveform for quick-response liquid powder displays," IEEE Trans. Consumer Electron **56**, 2043–2046 (2010).

[18] H. R. Kang, *Digital Color Halftoning* (SPIE Press, Bellingham, WA, 1999), pp. 171–196.

[19] T. Y. Park, I. S. Jang, and Y. H. Ha, "Banding artifact reduction with interweaving dot dispersion based on probability model and human visual system weighted root mean squared error in blue noise multilevel dithering," J. Imaging Sci. Technol. **53**, 1–13 (2009).

[20] N. Kaga, G. Yakushiji, H. Tazawa, M. Masutani, T. Kobayashi, T. Arai, K. Murata, R. Sakurai, Y. Kobayashi, H. Tamura, H. Anzai, H. Yamasaki, Y. Nishimuro, and K. Machida, US Patent 7,236, 291, Jun. 2007.